

# Optimisation of the parameters of an extended defect model applied to non-amorphizing implants

E. Lampin<sup>a,\*</sup>, F. Cristiano<sup>b</sup>, Y. Lamrani<sup>b</sup>, D. Connetable<sup>b</sup>

<sup>a</sup> IEMN/CNRS, Avenue Poincaré, 59652 Villeneuve d'Ascq Cedex, France

<sup>b</sup> LAAS/CNRS, 7 Avenue du Colonel Roche, 31077 Toulouse, France

## Abstract

In this paper, we present the optimisation of the parameters of a physical model of the kinetics of extended defects and applied the model with the optimised parameters to non-amorphizing implants. The model describes the small clusters, the {113} defects and the dislocation loops. In the first part, we determine the formation energies of the small clusters, the fault energy of the {113} defects, their Burgers vector and the self-diffusivity of silicon using TEM measurements and extractions of the supersaturation from the spreading of boron marker layers in low-dose implanted silicon. The improvements of the simulations are presented for the fitted experiments and for other wafers annealed at intermediate temperatures. In the second part, we increase the dose and energy of the non-amorphizing implant, leading to the transformation of {113} defects into dislocation loops. The predictions obtained with the optimised model are shown to be in agreement with the measurements.

*Keywords:* Model; Extended defects; Non-amorphizing implants

## 1. Introduction

The successful design of the future generations of transistors depends on the ability of process simulators to predict the transient enhanced diffusion (TED) of the dopants during post-implant annealing. Different groups [1–3] have investigated this phenomenon and shown that the TED is due to the supersaturation of self-interstitials maintained by extended defects. The extended defects form by agglomeration of excess self-interstitials initially created by the implantation process. They maintain a self-interstitial supersaturation in their vicinity during post-implant annealing. This supersaturation is at the origin of the enhanced diffusivity of dopants such as boron, which mainly diffuses via a self-interstitial mechanism [4]. It is thus crucial to predict the formation and evolution of extended defects during thermal treatments. The atom-by-atom models [5–8] of extended defects describe their formation by agglomeration of self-interstitials ( $\text{Si}_{\text{int}}$ ) through binary reactions of the type:



where  $(n)\text{Si}_{\text{int}}$  is a defect containing  $n$  atoms. In this work, this one step process is described according to the master equation:

$$\frac{dN_n}{dt} = F_{n-1}N_{n-1} - F_nN_n + R_{n+1}N_{n+1} - R_nN_n \quad (2)$$

where  $N_n(t)$  is the density of extended defects containing  $n$  atoms at time  $t$ .  $F_n$  and  $R_n$  are the forward and reverse rate of the reaction 1. Since the initial version of the model given by Cowern et al. [3], the expressions of  $F_n$  and  $R_n$  have been improved [6,9,10] to better describe the physical characteristics of the extended defects, ranging from the small clusters, to the {113} defects and to the dislocation loops. However, the numerical values of the fundamental parameters used in the model, namely the formation energies of the small clusters and the self-interstitial diffusivity, initially determined by Cowern et al. [3], and the fault energy and Burgers vector of the {113} defects from Colombeau et al. [9], have not been updated using the more complete description. Indeed, the results of the simulations may not be as satisfactory as it would be expected from the improvements of the physical description of the defects.

In this paper, we present the optimisation of the physical parameters of the improved description of the kinetics of extended defects using two sets of non-amorphizing low-dose implants [3,11]. Afterwards, the optimised model is tested on experiments [12] where the distance of the defects to the

\* Corresponding author. Tel.: +33 320197919; fax: +33 320197884.  
E-mail address: evelyne.lampin@isen.fr (E. Lampin).

surface, and the dose of the non-amorphizing implant are raised.

## 2. Optimisation of the model

A “simulated annealing” algorithm [13] is used to optimise the model. Simulated annealing tries to find the global optimum of a multi-dimensional function. It moves both up and downhill and as the optimization process proceeds, it focuses on the most promising area. This method ensures that the optimised values are independent of the particular initial set of parameters that are chosen. However, this procedure requires to run the simulation several hundreds to thousands of times. It is, therefore, a key issue to decrease the simulation time. The approach developed in reference [14] was used to reduce the number of equations by coupling the master Eq. (2) for the defects containing 2–12 atoms to a Fokker–Planck equation, the continuum version of the master equation, for the bigger defects (up to 30,000 atoms). This method has been shown to enable a drastic reduction of the computer time as far as small defects and  $\{113\}$  defects are concerned. This is exactly the case for the need of the present optimisation (see parameters to fit given above). The terms in the forward and reverse rate related to the dislocation loop creation, being well known from the literature [10], do not need to be optimised.

It was recently shown by Ortiz et al. [6] that, to extract a consistent set of physical parameters and eliminate unphysical solutions, it is essential to combine TEM measurements of the density of defects  $d_{\text{def}}$  and the mean number of atoms per defect  $n_{\text{def}}$  with supersaturation data  $S$  in the procedure of optimisation. Dedicated experiments (hereafter called “Cristiano’s experiments”) were carried on to measure  $d_{\text{def}}$ ,  $n_{\text{def}}$  and  $S$  on a single set of samples [11]. These samples are formed of two boron marker layers grown by CVD at a depth of 0.6 and 1.1  $\mu\text{m}$ , implanted with Si at 40 keV at a dose of  $6 \times 10^{13}$  ions/cm<sup>2</sup> and annealed in a furnace at 650, 700 and 740 °C and in rapid thermal annealing (RTA) at 815 °C. The mean number of atoms per defect  $n_{\text{def}}$  was fitted at the two extreme temperatures: 650 and 815 °C. The supersaturation  $S$  was also fitted, using a similar experiment published in reference [3] (hereafter called “Cowern’s experiments”). In this experiment, Si is self-implanted at  $2 \times 10^{13}$  ions/cm<sup>2</sup> and the same energy, and annealed by RTA at 600, 700 and 800 °C. The wider range of temperature variation (600–800 °C) allows a better quality of the optimisation. The values of  $S$  at 600 and 800 °C were used for the fit. In both Cristiano’s and Cowern’s experiments, the self-implantations are non-amorphizing and the extended defects are observed at 100 nm from the surface.

Figs. 1 and 2 show the results of the simulation with the default set of parameters and their optimised values. The points are extracted from the diffusion of the boron marker layers as far as the supersaturation values are concerned and from TEM measurements to get the mean number of atoms per defect ( $n_{\text{def}}$ ). The optimisation leads to slightly better results of the supersaturation at 600 and 800 °C. Moreover, the results predicted at 700 °C are also better than with the default set of parameters. However, the improvements are more evident for the mean num-

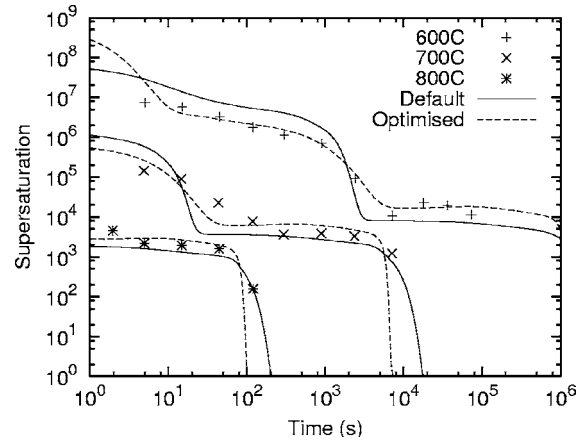


Fig. 1. Supersaturation of self-interstitials as a function of the annealing time. The points are obtained from Cowern’s experiments. The solid lines give the results with the default parameters (reference [3]). The dashed lines give the results with the optimised parameters obtained in the current work.

ber of atoms per defect (Fig. 2), although this characteristics of the defects is the most difficult to obtain quantitatively. However, Fig. 2 shows that the shape of the number of atoms as a function of the annealing time is better given. For the two intermediate temperatures (700 and 740 °C), the prediction is again closer to the experimental values than using the default parameters.

The formation energies of the small clusters and of the  $\{113\}$  defects extracted from the fit are given in Table 1 and Fig. 3. The energies of the defect containing 2–10 atoms exhibit the same oscillating behaviour as a function of the number of atoms than the extractions of Cowern [3] and Ortiz [6]. Two minima of energy are found as in the above extractions, their position in term of number of atoms are only slightly different due to the differences in the forward and reverse reaction rate [3] and in the implementation of the model [6]. The other fitted parameters, i.e. the Burgers vector (1.17 Å) and fault energy of the  $\{113\}$  defects (0.38 eV) and the self-diffusivity of the Si interstitials

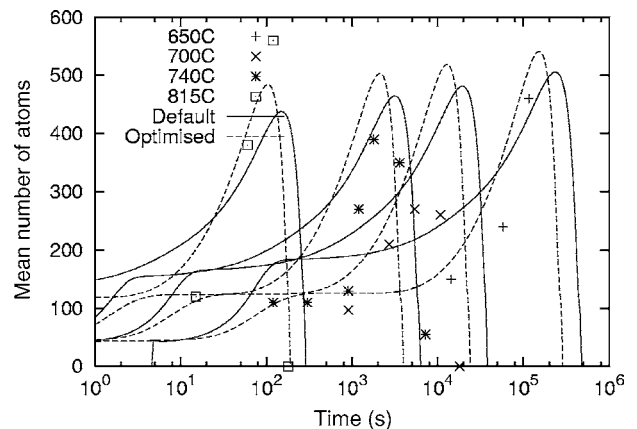


Fig. 2. Mean number of atoms per defect as a function of the annealing time. The points are obtained from Cristiano’s experiments. The solid lines give the results with the default parameters (reference [3]). The dashed lines give the results with the optimised parameters obtained in the current work.

Table 1

Formation energies of the small clusters, vs. the number of atoms in the defect, extracted from the fit

$n$	Formation energy (eV)
2	1.50
3	1.50
4	1.39
5	0.92
6	1.50
7	1.04
8	1.08
9	1.40
10	1.20

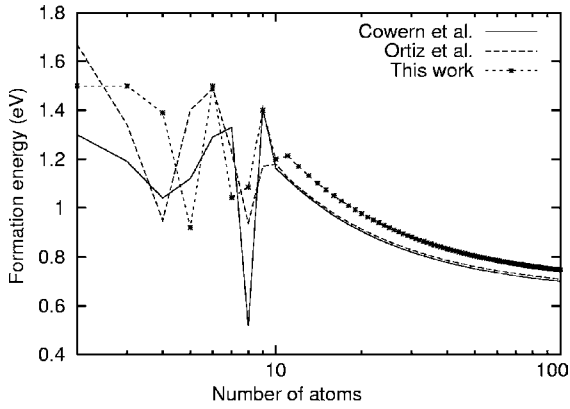


Fig. 3. Formation energies of the small extended defects. The solid line gives the default parameters of the model taken from reference [3]. The dashed line is an optimisation of the same model in a 1D implementation [6]. The joined points give the results of the present optimisation.

$(1.86 \times 10^{24} \text{ cm}^{-1} \text{ s}^{-1} \exp(-4.53 \text{ eV}/k_B T))$  are not significantly altered by the optimisation; the main degrees of freedom of the model are the free energies of the small clusters.

We have further tested the optimised model on the supersaturation of self-interstitials extracted from the Cristiano’s experiment. These values were not included in the fitted data base. Fig. 4 presents the results of the model with the default and optimised sets of parameters. The improvement is not spectacular but is evident. We can thus conclude that our physical model of the extended defects is now able to describe quantitatively the supersaturation of self-interstitials and the characteristics of the defects and test its predictions on new experiments.

### 3. Application of the optimised model to new experiments

In this second part, the experiment of reference [12], hereafter called “Calvo’s experiment” is simulated. In this experiment, Si is self-implanted at a dose of  $2 \times 10^{14} \text{ ions/cm}^2$  and an energy of 100 keV. Upon annealing at 850 °C, the extended defects will thus form at a larger distance from the surface: 0.25  $\mu\text{m}$  instead of 100 nm in the former experiments. The conditions of implantation and annealing are chosen to cause the transformation of  $\{113\}$  defects into dislocation loops at long annealing.

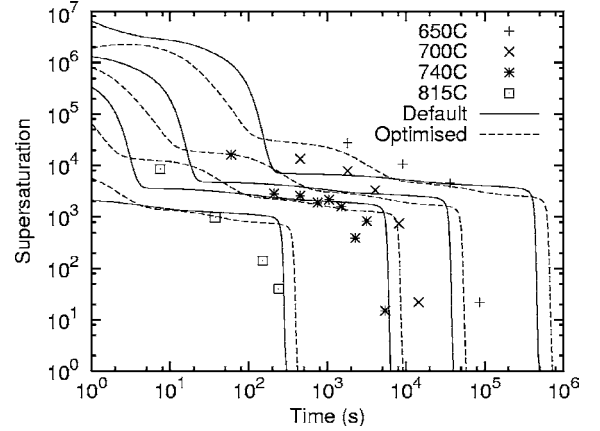


Fig. 4. Supersaturation of self-interstitials as a function of the annealing time. The points are obtained from Cristiano’s experiments. The solid lines give the results with the default parameters (reference [3]). The dashed lines give the results with the optimised parameters obtained in the current work.

The presence of dislocation loops is actually confirmed by TEM observations. As far as Si self-interstitial evolution is concerned, the supersaturation is extracted from the spreading of four boron marker layers. The experimental set up is detailed in the reference [11]. These experimental values are the joined points with error bars in Fig. 5. The results of two kinds of simulations are also presented in Fig. 5: with one type of extended defects for a large number of atoms, i.e. the  $\{113\}$  defects, in the first case and with a transition from  $\{113\}$  defects to dislocation loops in the second case at a size of approximately 400 atoms. In the first case, we obtain an abrupt fall (solid line in Fig. 5) of the supersaturation of self-interstitials at the time where the  $\{113\}$  defects dissolve. In the second case where dislocation loops are described, the supersaturation level decreases continuously with annealing time due to the progressive defect transformation. As expected, the variation of the supersaturation simulated with the dislocations loops is in closer agreement with the experimental

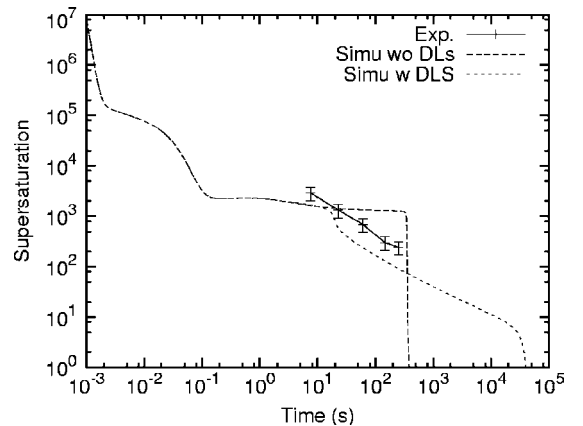


Fig. 5. Supersaturation of  $\text{Si}_{\text{ints}}$  as a function of the annealing time at 850 °C. The joint points with error bars are the results from Calvo’s experiments (“Exp.”). The solid line is the result of the simulation without the description of dislocation loops (“Simu wo DLS”). The short-dashed line is the result of the simulation including the description of dislocation loops (“Simu w DLS”).

behaviour. The conclusion is that the model of the kinetics of small clusters,  $\{113\}$  defects and dislocation loops, with optimised values of the small cluster and  $\{113\}$  defect parameters, is transferable to experiments where the conditions are considerably different from the fitting database.

#### 4. Conclusion

In this paper, we have presented the optimisation of our model of the kinetics of extended defects using the supersaturation of self-interstitials and the mean number of atoms in an extended defect to rule out unphysical parameters. The improvement is demonstrated on the values of the supersaturation and on the mean number of atoms in the  $\{113\}$  defects. The predictivity of the model is then tested. In a first time, the simulations are shown to be in agreement with the low-dose experiments. In a second time, the dose and energy are increased to form  $\{113\}$  defects and dislocation loops far from the surface. The results of the simulations are in this case also in close agreement with the experiment. The various tests demonstrate that the model is now quantitatively predictive.

#### Acknowledgement

This work is part of the Integrated Project NanoCMOS funded by the European Community.

#### References

- [1] D.J. Eaglesham, P.A. Stolk, H.J. Gossmann, J.M. Poate, *Appl. Phys. Lett.* 65 (1994) 2305.
- [2] A. Claverie, L.F. Giles, M. Omri, B. de Mauduit, G. Ben Assayag, D. Mathiot, *Nucl. Instr. Methods Phys. Res. B* 147 (1999) 1.
- [3] N.E.B. Cowern, G. Mannino, P.A. Stolk, F. Roozeboom, H.G.A. Huizing, J.G.M. van Berkum, et al., *Phys. Rev. Lett.* 82 (1999) 4460.
- [4] P.M. Fahey, P.B. Griffin, J.D. Plummer, *Appl. Phys. Lett. Rev. Mod. Phys.* 61 (1989) 289.
- [5] A. Claverie, B. Colombeau, B. de Mauduit, C. Bonafos, X. Hebras, G. Ben Assayag, et al., *Appl. Phys. A* 76 (2003) 1025.
- [6] C.J. Ortiz, P. Pichler, T. Fiihner, F. Cristiano, A. Claverie, B. Colombeau, N.E.B. Cowern, *J. Appl. Phys.* 96 (2004) 4866.
- [7] A.H. Gencer, S.T. Dunham, *J. Appl. Phys.* 81 (1997) 631.
- [8] M. Jaraiz, et al., *Mat. Res. Soc. Symp. Proc.* 532 (1998) 43.
- [9] B. Colombeau, F. Cristiano, A. Altibelli, C. Bonafos, G. Ben Assayag, A. Claverie, *Appl. Phys. Lett.* 78 (2001) 940.
- [10] F. Cristiano, J. Grisolia, B. Colombeau, M. Omri, B. de Mauduit, A. Claverie, F. Giles, N. Cowern, *J. Appl. Phys.* 87 (2000) 8420.
- [11] F. Cristiano, N. Cherkashin, X. Hebras, P. Calvo, Y. Lamrani, E. Scheid, B. de Mauduit, W. Lerch, S. Paul, A. Claverie, *Nucl. Inst. Methods Phys. Res. B* 216 (2004) 46.
- [12] P. Calvo, A. Claverie, N. Cherkashin, B. Colombeau, Y. Lamrani, B. de Mauduit, F. Cristiano, *Nucl. Inst. Methods Phys. Res. B* 216 (2004) 173.
- [13] A. Corana, M. Marchesi, C. Martini, S. Ridella, *ACM Trans. Math. Software* 13 (1987) 262.
- [14] E. Lampin, C.J. Ortiz, N.E.B. Cowern, B. Colombeau, F. Cristiano, *Solid State Electron.* 49 (2005) 1168.